Structure of Hybrid Polyhedral Oligomeric Silsesquioxane Polymethacrylate Oligomers Using Ion Mobility Mass Spectrometry and Molecular Mechanics

*Stanley E. Andersona, Erin Shammel Baker, Connie Mitchell, Timothy S. Haddad[b] and Michael T. Bowers**

Department of Chemistry & Biochemistry, University of California, Santa Barbara, CA 93106

[a]Department of Chemistry, Westmont College, Santa Barbara, CA 93108.

[b]ERC Inc., Air Force Research Laboratory, 10 East Saturn Boulevard, Building 8451, Edwards AFB, CA 93524-7680

RECEIVED DATE (to be automatically inserted after your manuscript is accepted if required according to the journal that you are submitting your paper to)

TITLE RUNNING HEAD Structure of Polyhedral Oligomeric Silsesquioxane Polymethacrylate (POSS) Oligomers

CORRESPONDING AUTHOR FOOTNOTE

* Corresponding author: Phone: 805-893-2893. Email: bowers@chem.ucsb.edu

[a] Westmont College

[b] ERC, Inc.

Report Documentation Page

Form Approved
OMB No. 0704-0188

1. REPORT DATE	2. REPORT TYPE	3. DATES COVERED
DEC 2004		**-**

4. TITLE AND SUBTITLE
Structure of Hybrid Polyhedral Oligomeric Silsesquioxane Polymethacrylate Oligomers Using Ion Mobility Mass Spectrometry and Molecular Mechanics

5a. CONTRACT NUMBER

5b. GRANT NUMBER

5c. PROGRAM ELEMENT NUMBER

6. AUTHOR(S)
Timothy Haddad; Stan Anderson; Erin Baker; Connie Mitchell; Mike Bowers

5d. PROJECT NUMBER
2303

5e. TASK NUMBER
0521

5f. WORK UNIT NUMBER

7. PERFORMING ORGANIZATION NAME(S) AND ADDRESS(ES)
Air Force Research Laboratory (AFMC),AFRL/PRSM,10 E. Saturn Blvd.,Edwards AFB,CA,93524-7680

8. PERFORMING ORGANIZATION REPORT NUMBER

9. SPONSORING/MONITORING AGENCY NAME(S) AND ADDRESS(ES)

10. SPONSOR/MONITOR'S ACRONYM(S)

11. SPONSOR/MONITOR'S REPORT NUMBER(S)

12. DISTRIBUTION/AVAILABILITY STATEMENT
Approved for public release; distribution unlimited

13. SUPPLEMENTARY NOTES

14. ABSTRACT

Ion mobility and molecular modeling methods were used to examine the gas phase conformational properties of POSS (Polyhedral Oligomeric Silsesquioxanes) propylmethacrylate (PMA) oligomers. MALDI was utilized to generate sodiated [(PMA)Cp7T8]xNa+ ions, and their collision cross-sections were measured in helium using ion mobility based methods. Results for x = 1, 2, and 3 were consistent with only one conformer occurring for the Na+1-mer and Na+3-mer, but two or more conformers are present for the Na+2-mer. Theoretical modeling of the Na+1-mer using the AMBER suite of programs indicates only one family of low-energy structures is found, in which the sodium ion binds to the carbonyl oxygen on the PMA and 4 oxygens on one face of the POSS cage. The calculated cross-section of this family agrees very well with the experimental value, with <2% deviation. For the Na+2-mer, theory predicts three separate conformer families based on whether the backbone attachments to the two POSS cages are "cis" (larger) or "extended trans" or "trans" (smaller). The calculated cross-sections agree very well with the two experimental values. For the Na+3-mer, theory predicts a "syndiotactic" family of structures at lowest energy whose average cross-section is consistent with the experimental cross-section. Modeling shows the different conformer families are primarily due to non-bonded interactions of the capping Cp groups which stabilize POSS cage packing in a variety of ways.

15. SUBJECT TERMS

16. SECURITY CLASSIFICATION OF:			17. LIMITATION OF ABSTRACT	18. NUMBER OF PAGES	19a. NAME OF RESPONSIBLE PERSON
a. REPORT	b. ABSTRACT	c. THIS PAGE			
unclassified	**unclassified**	**unclassified**		**26**	

Abstract

Ion mobility and molecular modeling methods were used to examine the gas phase conformational properties of POSS (Polyhedral Oligomeric Silsesquioxanes) propylmethacrylate (PMA) oligomers. MALDI was utilized to generate sodiated $[(PMA)Cp_7T_8]_xNa^+$ ions, and their collision cross-sections were measured in helium using ion mobility based methods. Results for x = 1, 2, and 3 were consistent with only one conformer occurring for the Na^+1-mer and Na^+3-mer, but two or more conformers are present for the Na^+2-mer. Theoretical modeling of the Na^+1-mer using the AMBER suite of programs indicates only one family of low-energy structures is found, in which the sodium ion binds to the carbonyl oxygen on the PMA and 4 oxygens on one face of the POSS cage. The calculated cross-section of this family agrees very well with the experimental value, with <2% deviation. For the Na^+2-mer, theory predicts three separate conformer families based on whether the backbone attachments to the two POSS cages are "cis" (larger) or "extended trans" or "trans" (smaller). The calculated cross-sections agree very well with the two experimental values. For the Na^+3-mer, theory predicts a "syndiotactic" family of structures at lowest energy whose average cross-section is consistent with the experimental cross-section. Modeling shows the different conformer families are primarily due to non-bonded interactions of the capping Cp groups which stabilize POSS cage packing in a variety of ways.

KEYWORDS POSS, Polyhedral oligomeric silsesquioxane (POSS), ion mobility, hybrid inorganic/organic

Stanley E. Anderson, Erin Shammel Baker, Connie Mitchell, Timothy S. Haddad and Michael T. Bowers*

Chem. Mater. **xxxx**, *xx*, xxxx

Structure of Hybrid Polyhedral Oligomeric Silsesquioxane Polymethacrylate Oligomers Using Ion Mobility Mass Spectrometry and Molecular Mechanics

The theoretically modeled syndiotactic isomer of $[(PMA)Cp_7T_8]_3$ oligomer (Cp = cyclopentyl omitted) shows the POSS cages close-packed along the PMA backbone. The Na^+ (yellow) is coordinated to 3 carbonyl oxygens (red) and 4 oxygens of a cage face. The experimental collision cross-section was 539 $Å^2$, compared to the calculated cross-section of 540 $Å^2$.

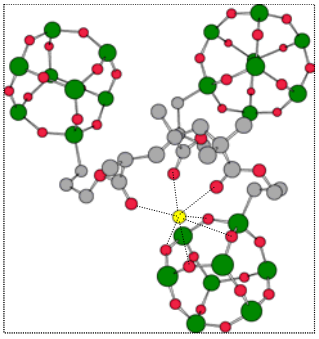

Introduction

The ability to enhance properties of materials for increased performance and environmental robustness is the focus of much current research. One approach to developing better materials is to create inorganic-organic composite materials in which inorganic building blocks are incorporated into organic polymers. Polyhedral Oligomeric Silsesquioxanes (POSS) are one type of hybrid inorganic/organic material of the form $(RSiO_{3/2})_n$, or R_nT_n, where organic substituents are attached to a silicon-oxygen cage.[1] The most common POSS cage is the T_8 (eg., Me_8T_8 in Figure 1), although other cages with well-defined geometries include n = 6, 10, 12, 14, 16 and 18.[2,3] By incorporating these Si-O cages into organic polymers, properties superior to the organic material alone are realized, offering exciting possibilities for the development of new materials.

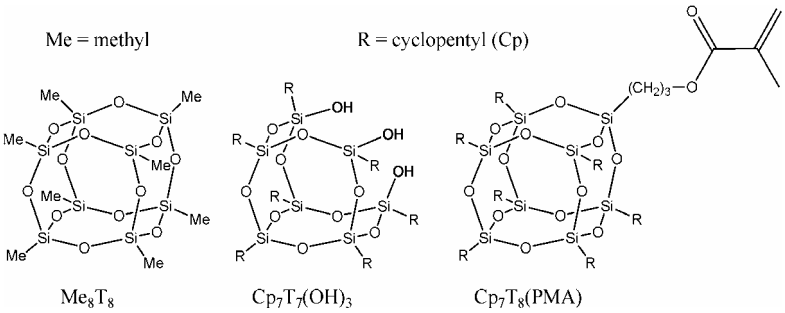

Figure 1. Three common POSS materials: A fully condensed cage with eight methyl groups (Me_8T_8), an incompletely condensed trisilanol ($Cp_7T_7(OH)_3$) useful in making a polymerizable POSS with a single functionality; and a Cp_7T_8(propylmethacrylate).

The first synthesis of POSS began in the 1940's[4] when Scott isolated the highly symmetric Me_8T_8. However, it was not until 1955 that proper characterization occurred with X-ray crystallography.[5] Significant synthetic advances were made in 1989 when Feher[6] improved on earlier synthetic methods[7] to make well-defined incompletely condensed POSS (e.g. $Cp_7T_7(OH)_3$ in Figure 1),

which permitted the easy synthesis of polymerizable POSS such as $Cp_7T_8(R')$ where R′ is a functionality like propylmethyacrylate,[8] norbornene,[9] or styrene.[10] In 1993 the first POSS polymers were synthesized[11] using $Cp_7T_8(R')$ units. Functionalized POSS are more elegantly incorporated into thermoplastics by copolymerization than by mere blending to yield a nanocomposite. Chemically bonded POSS can either dangle from, or be part of the polymer backbone. Currently, light weight, high-temperature plastics, lubricants, insulation and materials resistant to atomic oxygen have employed POSS polymers, and a great deal more research is being conducted on POSS polymer systems as indicated by the many review articles published. [12-16]

Of major interest is how the cage structures affect the polymer to which they are attached. An emerging theme from numerous papers indicates that POSS groups undergo self-assembly/association to form POSS-rich domains that strongly affect polymer properties.[8-11,17-23] This association has been observed both by X-ray scattering and TEM. A recent paper terms this a "bottom-up" approach to nanocomposite formation, where the POSS aggregate together to form rafts and sheets within a polymer matrix.[23]

To create improved POSS-containing polymers on any basis other than trial and error, structure-property relationships for a variety of POSS-containing thermoplastics must by thoroughly understood. It is often not known where the POSS cages are attached (end, middle, etc.), how the polymer conformation changes to adapt to the POSS, how far apart the POSS cages are, or how any of these issues affect the microstructure and particular property of interest. Being able to understand the detailed information about how POSS groups interact within an oligomer of known length is essential to creating better polymers.

A technique which incorporates mass spectrometry, ion mobility, and theoretical modeling has been developed in our group to analyze ions based on their mass and conformational size. Many POSS monomers with a variety of functional groups have been successfully measured and modeled using this technique.[24] For example, $Na^+Sty_8T_8$ was studied in great detail and different conformational families

were found based on the number of styryl group pairs that occur. Ion mobility cross-sections, theoretical cross-sections and those calculated from the X-ray structures were all in excellent agreement.[25] In a recent study of the epoxy-styryl system, $Na^{+}Sty_{8-x}Ep_xT_8$ (x = 1,2,3),[26] isomers were separated by ion mobility and examined with molecular modeling, again yielding theoretical results within 1-2% of experiment. These monomer results give us confidence that this method can be applied to POSS oligomers, especially since our early work on the conventional polymers PEG,[27] PPG,[28] and PTMG,[29] poly(ethyleneterephthalate) PET,[30] poly(methylmethacrylate)(PMA),[31] and poly(styrene)[32] was successful in elucidating their structures.

The synthesis and bulk properties of POSS cages capped with one PMA to form the polymer backbone and seven organic groups ($[(PMA)R_7T_8]_x$) have been studied as homopolymers[8] (shown in Figure 2) and as cross-linked copolymers.[15,20] $[(PMA)R_7T_8]_x$ form amorphous, brittle plastics with very high thermal stabilities, but a lack of structural information prevents any real understanding of the dramatic role of the POSS moiety in modifying acrylics other than the suggestion that the POSS pendant increases the rigidity of the polymer backbone. Ion mobility[31] and mass spectrometry[33] studies in our laboratory on PMA from the 3-mer to the 11-mer with no POSS attached showed that the metal ion used to cationize the species binds to the ends of the oligomers forming very stable cyclic structures reminiscent of crown ethers. Up to six oxygens from the carbonyl groups coordinate to the cation. It was determined that the choice of cation and nature of the PMA end groups have a significant influence on how strongly the cation binds to the oligomer backbone and alters the conformational preference of the oligomers. This paper reports for the first time how the POSS cage location plays a significant role in the resulting structure of the $[(PMA)Cp_7T_8]_x$ oligomers for x=1-3, and addresses the issue of whether the sodium cation affects the observed structures.

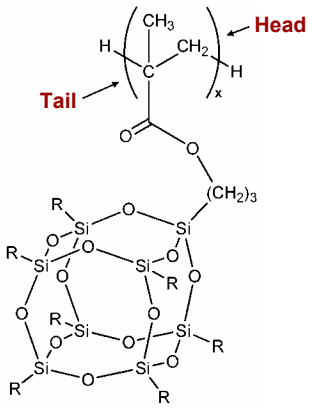

Figure 2. A homopolymer of a POSS-propylmethacrylate terminated at both ends with hydrogens.

Experimental

Synthesis and Isolation of POSS oligomers

To promote the formation of POSS oligomers, a variety of different polymerizations were carried out using varying amounts of free radical initiator azoisobutylnitrile (AIBN). The best results were obtained using a 0.5 molar solution of monomer with 2 mole % AIBN free radical initiator. A flask containing 1.002 g (0.975 mmole) of $(c\text{-}C_5H_9)_7[Si_8O_{12}](CH_2CH_2CH_2OC(=O)C(CH_3)=CH_2)$, 3.6 mg (0.022 mmole) of AIBN initiator, and 1.7 g toluene was sealed under nitrogen and heated to 70 ˚C for 1 day. To isolate the product, this solution was diluted with 3 mL of $CHCl_3$ and added to methanol (10 mL). The precipitate (containing mostly polymer) was filtered off and the filtrate (containing mostly monomer and short oligomers) was evaporated to dryness. This dried $[(PMA)Cp_7T_8]_x$ filtrate was used to obtain the mass spectra and arrival time distributions (ATDs) discussed in this paper.

Ion Mobility/Mass Spectrometry

A home-built MALDI-TOF instrument was utilized in performing experimental analysis on the $[(PMA)Cp_7T_8]_x$ POSS sample. The details regarding the experimental setup for the mass spectrum and ion mobility measurements have previously been published,[25, 34-36] so only a brief description will be given. Sodiated $[(PMA)Cp_7T_8]_x$ ions were formed by MALDI in a home-built ion source. 2,5-dihydroxybenzoic acid (DHB) was used as the matrix and tetrahydrofuran (THF) as the solvent. Approximately 50 μL of DHB (100 mg/mL), 50 μL of the POSS sample (1 mg/mL) and 8 μL of NaI (saturated in THF) were applied to the sample target and dried. A nitrogen laser (λ=337 nm, 12 mW power) was used to generate ions, using MALDI methods, in a two-section (Wiley-McLaren) ion source. The ions were accelerated with 9kV of acceleration voltage down a 1-meter flight tube and encountered a reflecting lens where they were redirected and reaccelerated to a detector. The result is a high-resolution mass spectrum of the ions formed in the source. In order to perform ion mobility experiments, the reflectron was switched off and the TOF operated in a linear mode using a mass gate. The mass selected ions are decelerated and gently injected into a 20-cm long glass drift cell filled with

~1.5 torr of helium gas where they drift under the influence of a weak electric field. The temperature of the cell can be varied from 80K to 500K. After exiting the drift cell, the ions pass through a quadrupole mass filter and are detected.

A timing sequence is initiated by the extraction pulse in the ion source. Ions are detected as a function of time at the detector generating an arrival time distribution (ATD). The important part of the arrival time (t_A) is the time the ion packet spends in the drift cell undergoing collisions with the background gas. These collisions, and the electric field E in the cell, generate a constant drift velocity v_d,

$$v_d = KE = K_o E \frac{760}{p} \frac{T}{273.16} \tag{1}$$

where the constant K is termed the mobility and K_o the reduced mobility at standard temperature T and pressure p. The arrival time is given by

$$t_A = \frac{l^2}{K_o} \frac{1}{760} \frac{273}{T} \left(\frac{p}{V} \right) + t_o \tag{2}$$

where V is the voltage across the cell, l is the cell length and t_o the time the ions spend outside the drift cell before being detected. A plot of t_A vs p/V yields a straight line with intercept t_o and a slope proportional to $1/K_o$. Using kinetic theory[37] it is straightforward to obtain the cross-section from K_o

$$\sigma = \frac{3q}{16NK_o} \left(\frac{2\pi}{\mu k_b T} \right)^{1/2} \tag{3}$$

where q is the ion charge, N is the gas density in the cell, μ the ion-He reduced mass, and k_b the Boltzmann's constant.

Theoretical Modeling

The AMBER suite of molecular mechanics/molecular dynamics (MM/MD) programs[38] is used to generate families of low-energy structures. We have developed an annealing protocol that involves repeated cycles of high temperature heating, cooling and energy minimizing. From this procedure we obtain cross-sections and relative energies of 100 to 200 candidate structures (a so-called scatter plot). In almost all cases we obtain agreement of 1-2% between experimental cross-sections and averaged low energy model cross-sections.

The $[(PMA)Cp_7T_8]_x$ POSS oligomer systems present large challenges both experimentally and theoretically. We developed AMBER parameters for Si from the ab-initio calculations of Sun and Rigby[39,40] that were designed to provide force field parameters for polysiloxanes and have updated and expanded this parameter database using recent crystal structure data[41,42] which give more accurate Si-O and Si-C distances. We use the commercially available Hyperchem[43] program to build starting structures for AMBER and then to view and visually classify the calculated minimum energy structures. In order to get a "better" structural sampling of phase space, we increased the annealing temperature from the customary 800 K to 1400 K. Exponential cooling to 50 K was used rather than linear cooling before energy minimization to get the final structure. To ensure that the cation did not dissociate by metal ion loss at 1400 K, a built-in AMBER distance restraint was used.

Calculating cross-sections from model structures can be difficult in the size range of the oligomers studied here. The modified projection method[27,37] has been found to provide accurate cross-sections for systems with masses below about 1500 Daltons. However, for systems above about 1500 Daltons this method appears to progressively underestimate the true cross-section, presumably because multiple ion-He encounters occur in a given collision. The more spherical the molecule the better job it does. More rigorous trajectory methods have also been developed.[44,45] In the simpler of these, a hard

sphere interaction potential is used.[44] This model works well for large systems with masses greater than 10,000 Daltons but systematically overestimates the cross-sections for smaller systems. When a Lennard-Jones interaction potential is included[45] better results are obtained but this method at times overestimates cross-sections in the intermediate 1500 to 5000 Dalton mass range depending on the type of structure being analyzed.[46] These issues do not seriously impact the interpretation of any of the systems studied here.

Results and Discussion

The MALDI-TOF mass spectrum of the sodiated $[(PMA)Cp_7T_8]_x$ oligomers is shown in Figure 3. The peaks for x = 2 and x = 3 appear at the exact masses corresponding to the sodiated 2-mer and 3-mer. Higher oligomers, at least up to the 4-mer and 5-mer, are present but in such small quantities that it is not possible to obtain arrival time distributions. ATDs for the $[(PMA)Cp_7T_8]_xNa^+$ oligomers were recorded both at 300 K and at 80K, with only a slight narrowing of the peaks observed at 80 K but no qualitative differences.

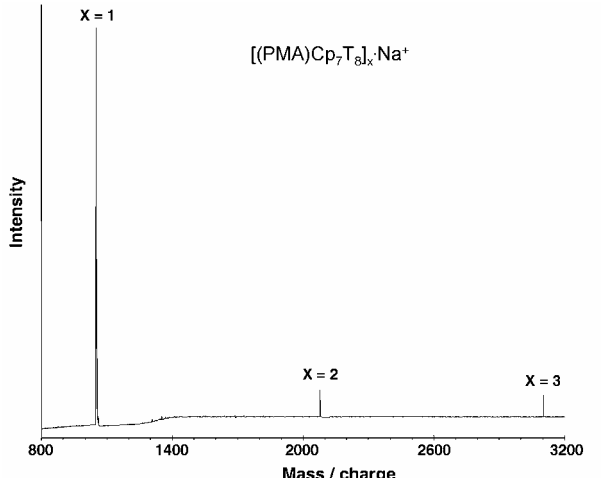

Figure 3. MALDI-TOF mass spectrum of $[(PMA)Cp_7T_8]_x{\cdot}Na^+$ oligomers.

1-mer

The ATDs for the masses corresponding to the three peaks observed in the mass spectrum are shown in Figure 4. The ATD for the 1-mer shows a single Gaussian peak with a linewidth consistent with a single species. An experimental cross-section of 248 $Å^2$ was obtained. Figure 5 shows a cross-section versus relative energy "scatter plot" of the calculated cross-sections of 100 structures obtained from the annealing protocol. Since all 100 energies fall within a relative energy 2.5 kcal/mol, the cross-section reported in Table 1 is an average of all the cross-sections for this "family" of structures. This value agrees with the experimental cross-section within 2%, which is typical based on the many POSS

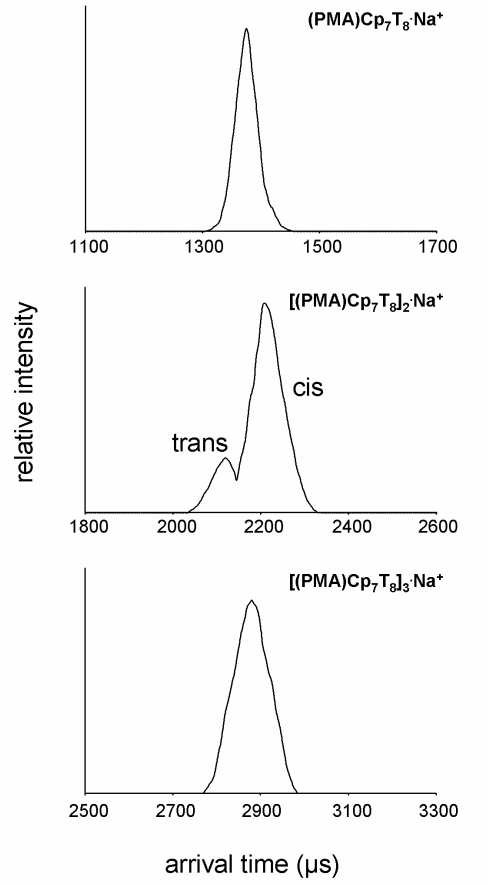

Figure 4. Arrival time distributions (ATDs) of $[(PMA)Cp_7T_8]_x{\cdot}Na^+$ for x = 1, 2, 3 obtained at a drift cell temperature of 300K. See text for "cis" and "trans" labeling for x = 2.

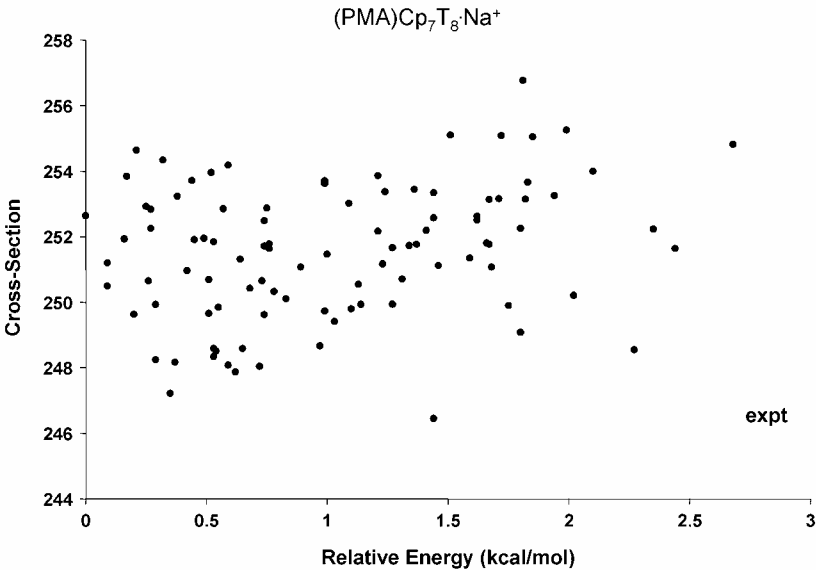

Figure 5. Plots of cross-section vs. energy for $(PMA)Cp_7T_8{\cdot}Na^+$. Each point represents one theoretical structure generated by the simulated annealing method. The average cross-section is based on all structures since the relative energies of these structures are very similar.

monomers we have previously measured and modeled.[24-26] The fact the calculated cross-sections are slightly systematically higher than experiment (Fig. 5) is probably not significant since the projection model should work well for molecules in this size range. Figure 6 shows a typical structure of the 1-mer. The sodium cation is coordinated to a carbonyl oxygen and four POSS cage face oxygens. A 5 (or 6) coordinate cation is a basic theme which will recur in the 2-mer and 3-mer structures.

2-mer

The ATD of the 2-mer shows two peaks indicating at least two distinct families of structures. The shorter time peak has a cross-section of 378 $Å^2$ and the longer time peak a cross-section of 402 $Å^2$. The scatter plot obtained from modeling the 2-mer is given in Figure 7. In this instance it is necessary to view the actual structure corresponding to each data point to determine if it belongs in a particular structural family. When this is done, it is apparent that three major structural groups are present, two of

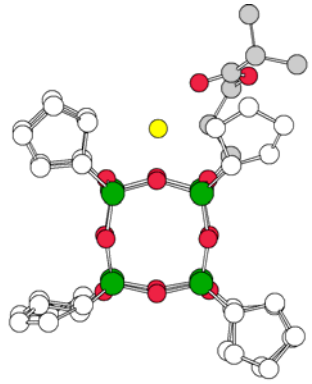

Figure 6. A typical structure calculated for (PMA)Cp_7T_8·Na^+. The cyclopentyl carbon atoms are white, the methacrylate group carbon atoms are gray, silicon is green, carbonyl and POSS oxygen atoms are red and sodium is yellow (hydrogen atoms have been omitted for clarity).

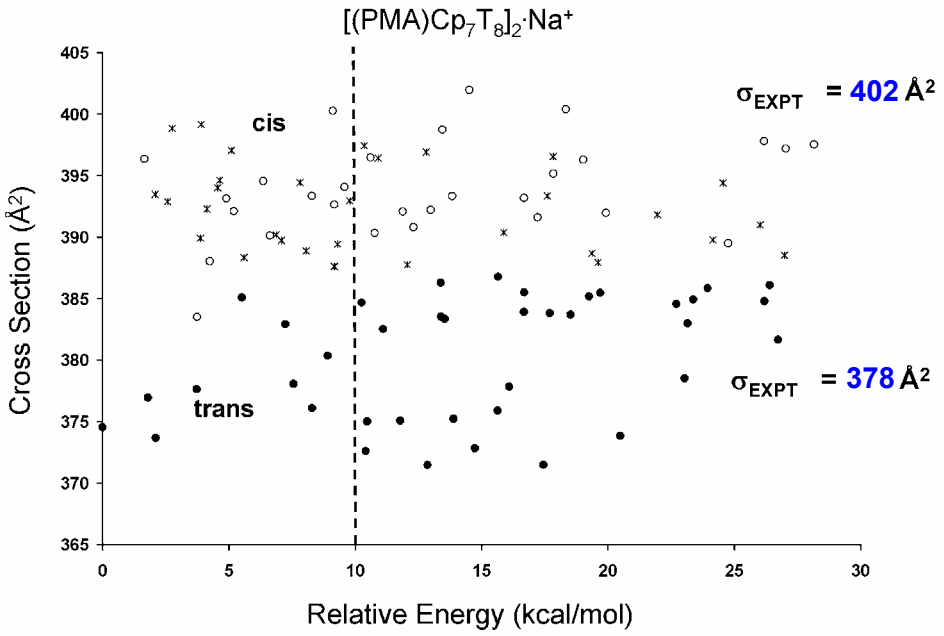

Figure 7. Scatter plot of cross-section vs. energy for [(PMA)Cp_7T_8]$_2$·Na^+. Each point represents one theoretical structure generated by the simulated annealing method. Minimum energy structures belonging to the trans family are closed circles (●), those in the extended trans family are x's (∗), and those belonging to the cis family are open circles (o).

which overlap and are virtually identical in cross-section. Representative structures of these three basic structural motifs are given in Figure 8, which we define as "cis" and "trans" and for reasons given below. The two experimental cross-sections are placed on the scatter plot in Fig. 7. There is good agreement of the smaller experimental cross-section with the "trans" family structures and the larger experimental cross-sections with the "cis" and "extended trans" families. Table 2 gives a breakdown of the average calculated cross-sections for modeled structures which lie in the relative energy ranges of 0 - 5 kcal/mol and 5 – 10 kcal/mol. The average cross-sections for "cis and "extended trans" conformers are so close that it is understandable why they cannot be resolved experimentally without a much higher resolution ion mobility cell. The calculated cross-section of the smaller trans conformer is within 1% of experiment; the larger "cis" and "extended trans" conformer cross-sections as a group are within ~2% of the experimental value.

We define "cis" and "trans" based on where the backbone is oriented relative to the adjacent POSS cages. The smaller "trans" conformer is characterized by a sodium cation coordinating to the 4 oxygen atoms on the face of a POSS cage and two carbonyl oxygens of the methacrylate group similar

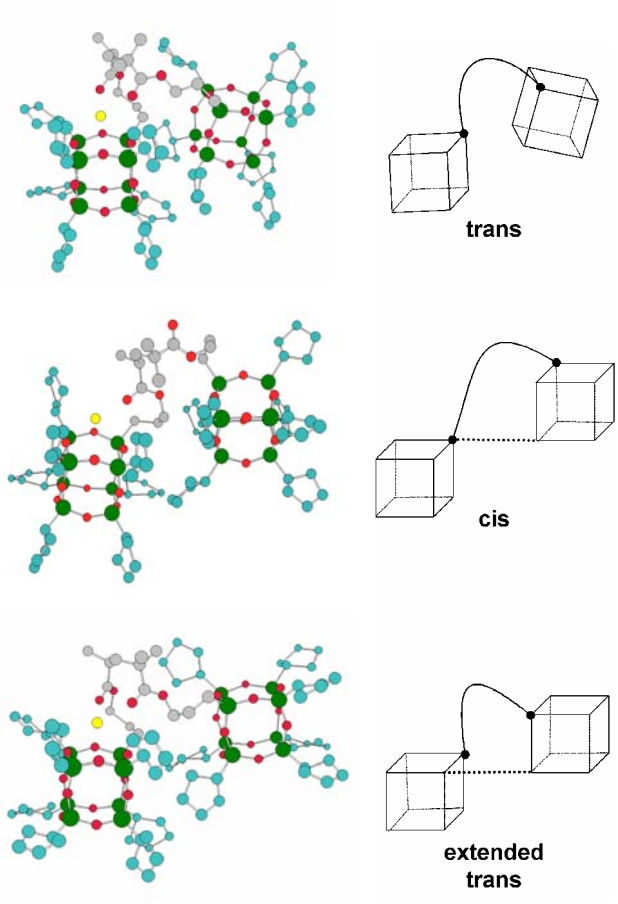

Figure 8. The lowest-energy structures calculated for the $[(PMA)Cp_7T_8]_2{\cdot}Na^+$. The sodium ion is shown for both structures and coordinates to a different number of oxygens in more compact versus less compact structures. The cyclopentyl groups capping the silicon atoms are omitted for clarity. The methacrylate group carbon atoms are gray, silicon is green, carbonyl and POSS oxygen atoms are red and sodium is yellow.

to the 1-mer. The second cage is aligned so that the faces of the two cages have a closest contact less than ~ 5.0 Å. The backbone bridges front-back cage vertices (Figure 8) and the Cp groups are splayed back away from the cage faces to make this close approach possible. The larger "cis" conformer shows the same 5 or 6-coordinate metal ion bonding as in the more compact "trans" structure, but the second cage has rotated by ~45° due to interfacial Cp group interactions, forcing the backbone into a back-back connectivity of the cages that increases the inter-cage separation to a mean value of ~6.3 Å. Similarly in the "extended trans" conformation, the Cp groups are positioned between the cages and force them apart to give an extended, but still trans-like cage connectivity. Thus the "cis" and "extended trans" conformers are characterized by more open structures.

Dynamics for 1 ns on the lowest energy representative cis/trans structures at 300K and 500K does not interchange the conformers, indicating a relatively high barrier to inter-conversion. At 800 K the trans structure maintains a constant cross-section, but the larger cis and extended trans conformers inter-convert to one another and to the smaller trans conformer. These structures when energy minimized, tend to fall in the higher relative energy side of the scatter plot. For example, the cation may be located *between* the two cage faces or may occupy a position with a lower coordination number on a face away from a backbone carbonyl group. The 20:80 distribution in the relative amounts of smaller to larger conformers, based on ATD peak intensity, is roughly the same ratio as the relative

number of structures found in the modeling process. This is believed to be mainly an entropy effect. There is simply a greater probability of having larger, more extended structures with more random possibilities for positioning the backbone chain, the cages themselves, and the cation.

The question arises about the importance of the cation in determining oligomer structures. We modeled the 2-mer without the cation present to explore this question. The interesting result is we get identical cis and trans families as found with the cation present, having cross-sections within experimental error of the observed value (see Table 1). This result strongly suggests that the families represent distinct cage packing made possible by specific backbone orientations. We conclude that the oligomer geometry is not being controlled by presence of the cation but by the way the POSS cages pack relative to the backbone.

The above discussion describes only head-to-tail bonding of the POSS units, where "head" refers to the terminal $=CH_2$ and "tail" refers to the POSS-bonded carbon end of the double bond in the monomer (see Figure 2). Modeling shows that it makes no difference whether the monomers come together to form head-tail, head-head or tail-tail isomers. Similar features and the same cis/trans conformers are observed in each isomer set. The identical size and similar orientation and relative location of the POSS cages themselves are the most important factors in determining the cross-section of the 2-mer.

3-mer

The 3-mer ATD is a single peak with no shoulders or other features apparent. Recording the ATD at 80K did not resolve any new peaks. Hence either a single structure is present, or more likely, there are unresolved isomeric structures of nearly identical cross-section since many are possible. The measured cross-section for the 3-mer is 539 $Å^2$.

Modeling of the 3-mer is more complicated than the 2-mer because of additional isomer possibilities. Figure 9 shows how monomers can condense to form the two regioisomers one expects for

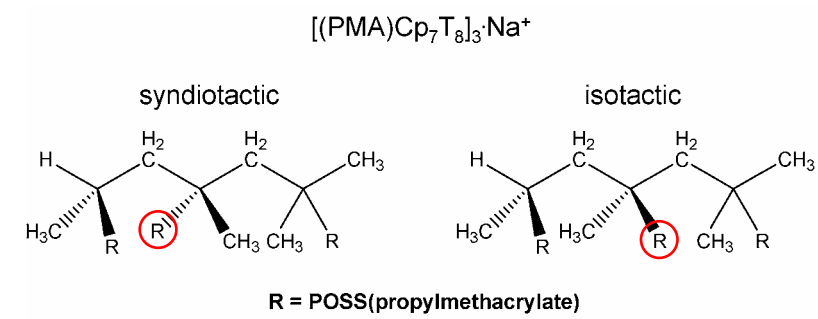

Figure 9. The $[(PMA)Cp_7T_8]_3{\cdot}Na^+$ oligomer (terminated at both ends with hydrogens) has two possible regioisomers. In a staggered conformation, the POSS groups (R) bonded to the two chiral centers are either syndiotactic (left) or isotactic (right) with respect to each other.

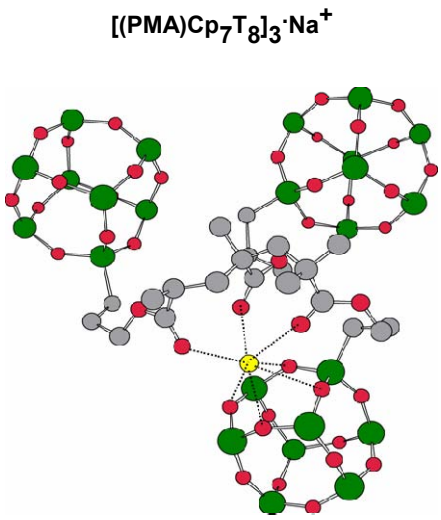

Figure 10. The lowest-energy structures calculated for the $[(PMA)Cp_7T_8]_3{\cdot}Na^+$ syndiotactic isomer. The sodium ion is typically coordinated to a cage face and one or more carbonyl oxygens of the oligomer backbone. The cyclopentyl groups capping the silicon atoms are omitted for clarity, the methacrylate group carbon atoms are gray, silicon is green, carbonyl and POSS oxygen atoms are red and sodium is yellow.

the hydrogen-terminated 3-mer, which is the species we observe in the mass spectrum. A typical lowest energy "syndiotactic" structure obtained from modeling is shown in Figure 10. The theoretical cross-section[45] of 540 Å^2 matches almost exactly the experimental value of 539 Å^2. This calculated cross-section is based on an average of all structures within the lowest 5 kcal of relative energy. On the other hand, a similar calculation for the isotactic structure is significantly larger at 555 Å^2 or about 3% larger than experiment. Comparing the entire scatter plots of cross-section versus relative energy, the centroid of syndiotactic structures is lower in cross-section than the centroid of the isotactic set by about 3%. We cannot categorically rule out the slightly larger isotactic isomer but the syndiotactic structure obviously fits experiment better.

Some generalizations can be made from either set of structures. First, the cation is at least 5-coordinate (as in the 1-mer and 2-mer) with carbonyl oxygens "pinning" the cation to a face of *one* of the cages. In the 3-mer the three POSS cages are in a more crowded environment than in the 2-mer because of the additional Cp capping groups. They tend to arrange themselves as far from one another as possible to minimize repulsions. The POSS cages are farther apart on average in both 3-mer isomers than in the 2-mer. Sharing a cation between cages introduces significant strain and is therefore a high energy structure. When it does occur, the third POSS cage is at relatively large distances from the

others (> 7 Å). This crowding of POSS cages is expected to become more important with increasing number of POSS units.

Finally, there is considerable spread in the relative energies of possible structures which differ mainly in the coordination environment of the metal ion. The angle of separation between the POSS cages seems to determine the cross-section. The most compact structures are lowest in energy and position the POSS cages in a near equilateral triangle. Higher energy structures are characterized by an opening of the angle formed by the centers of the POSS cages along the backbone. Relative head-tail connectivity of the 3-mer backbone makes very little difference in the calculated cross-sections; they all agree within experimental error. Consequently, such isomers cannot be resolved experimentally given the resolution of our current instrument.

If one models the 3-mer without the metal ion present as we did for the 2-mer, the minimum energy cross-section of the neutral species is virtually identical to the cationized form, supporting the conclusion that a metal ion has minimal effect on the backbone geometry and structure of the oligomer.

Larger systems

It has not yet been possible to obtain ATDs for oligomers larger than the 3-mer. Consequently, we are actually pursuing alternative methods of custom synthesis. Changing either the amount of AIBN in the standard free radical synthesis or the reaction time has not proved fruitful; we can detect higher oligomers via mass spectrometry but the intensities are very weak. Either the concentration of these oligomers is exceedingly small or their ionization efficiencies are very low. A better procedure for preparation of nearly pure designer oligomers may be to use "living polymer" methods of synthesis of the POSS-PMA's to make the 4-mer, 5-mer, 6-mer, etc., one unit at a time. The atom transfer procedure (ATRP)[47] is currently being attempted[48] to synthesize these species and possibly introduce an amino group on the terminus which should easily protonate to give an observable ion. We will report on these higher oligomers in the future.

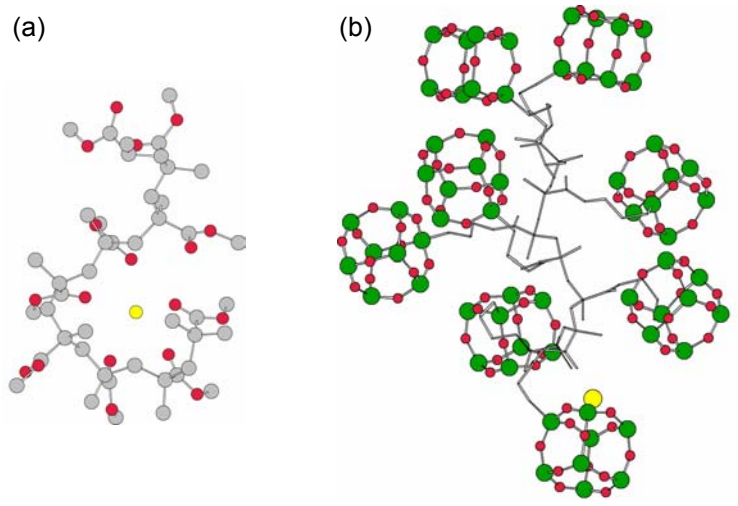

Figure 11. The lowest-energy structures calculated for a Na^+ cationized (a) 8-PMA and (b) POSS 8-PMA. The cyclopentyl groups capping the silicon atoms are omitted for clarity. The methacrylate group carbon atoms are gray, silicon is green, carbonyl and POSS oxygen atoms are red and sodium is yellow.

While we can draw certain simple conclusions about oligomer structure of these $[(PMA)Cp_7T_8]_x$ materials based on the 2-mer and 3-mer structural themes described above, we cannot definitively characterize the structural features of higher oligomers until experimental data becomes available. However, given the excellent agreement between experiment and theory for the 2-mer and 3-mer, we can use modeling to predict structural features for the higher oligomers with the expectation that experimental data will eventually become available. Figure 11, for example, compares the lowest energy, minimum cross-section structure of a non-POSS 8-PMA with the POSS 8-mer. The stereo view of the POSS 8-mer in Figure 12 has a perspective down the near-linear backbone axis. It is evident that the POSS groups are distributed in clusters of two or three or more (depending on the structure chosen) around the backbone axis exactly as in the 2-mer and 3-mer. Analyzing contributions to the total AMBER energy suggests that this type of clustering is clearly due to van der Waals nonbonded interactions between the R-groups on the cages and increases with the number of cages in the cluster. This may

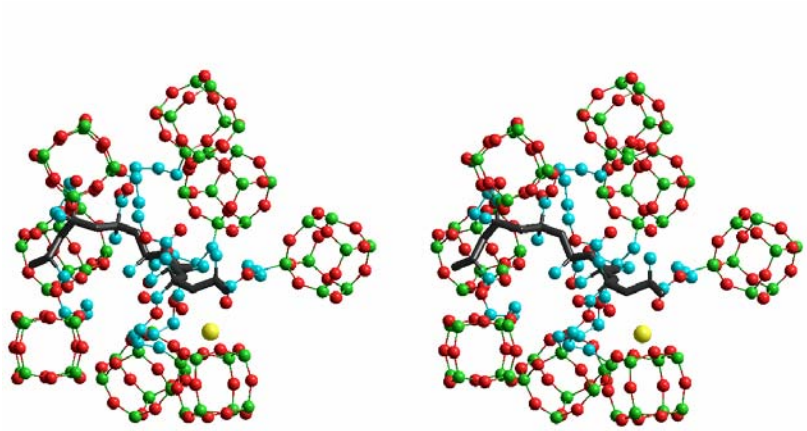

Figure 12. Stereoscopic view of the lowest-energy structure calculated for the $[(PMA)Cp_7T_8]_8$·Na+. The cyclopentyl groups capping the silicon atoms are omitted for clarity. The "backbone" carbon atoms rendered as tubular are black, all other carbons are blue, silicon is green, carbonyl and POSS oxygen atoms are red and sodium is yellow.

explain the failure of the 8-mer to add another monomer unit in the ARTP synthesis under the usual conditions.[48] The cluster becomes so stable at some point that it energetically and sterically inhibits reactivity with another large POSS monomer. We predict that new synthetic conditions such as much higher reaction temperatures may be needed to overcome this clustering tendency and make it possible for additional POSS units to attach. Figures 11 and 12 also show that the tether to the POSS cage is long enough to allow the first and last POSS units on the backbone to be held relatively close to one another due to clustering even though the backbone is essentially linear. The metal ion is typically associated with a single cage and one or two carbonyl groups as shown. This is a very different structure than the simple 8-PMA, in which the cation binds to 5 or 6 carbonyl groups of the backbone which is then forced to form crown-ether-like conformers as the dominant theme.

In summary, we have used ion mobility mass spectrometry to measure the cross-sections of the sodiated $[(PMA)Cp_7T_8]_x$ oligomers, where x = 1, 2, 3. Low energy structures obtained by molecular modeling agree with experiment within ~2%. Cis, trans, and extended trans structures of the 2-mer give rise to two groups of conformers. These structures seem to be determined primarily by non-bonded interactions of the cyclopentyl capping groups that cause the cages to pack in a variety of ways. The 3-mer structure is consistent with the syndiotactic regioisomer; it shows similar cage-cage-interactions due to non-bonded interactions. With the exception of the 1-mer, the presence of the cation does not influence the oligomer backbone structure like it does in the non-POSS oligomeric systems previously studied.

ACKNOWLEDGMENT

The Air Force Office of Scientific Research under grant F49620-03-1-0046 is gratefully acknowledged for support of this work. We also thank the NAS/NRC Senior Associateship Program for fellowship support of S.E.A.

REFERENCES

1. Voronkov, M.G.; Vavrent'yev, V.I. *Top. Curr. Chem*., **1982**, *102*, 199-236.

2. a) Agaskar, P.A. *Inorg. Chem*., **1993**, *30*, 2707-2708. b) Agaskar, P.A.; Klemperer, W.G. *Inorg. Chim. Acta*., **1995**, *229*, 355-364.

3. Franco, R. ; Kandalam, A.K. ; Pandey, R.; Pernisz, U.C. *J. Phys. Chem. B*, **2002**, *106*, 1709-1713.

4. Scott, D.W. *J. Amer. Chem. Soc*., **1946**, *68*, 356-358.

5. Barry, A.J.; Daudt, W.H.; Domicone, J.J.; Gilkey, J.W. *J. Amer. Chem. Soc*., **1955**, *77*, 4248-4252.

6. a) Feher, F.J.; Newman, D.A.; Walzer J.F. *J. Amer. Chem. Soc*., **1989**, *111*, 1741-1748. b) Feher, F.J.; Budzichowski, T.A.; Blanski, R.L.; Weller, K.J.; Ziller, J.W. *Organometallics*, **1991**, *10*, 2526-2528.

7. Brown, J.F.; Vogt, L.H. *J. Amer. Chem. Soc*., **1965**, *87*, 4313-4317.

8. Lichtenhan, J.D.; Otonari, Y.; Carr, M.J. *Macromolecules,* **1995,** *28*, 8435-8437.

9. Jeon, H.G.; Mather P.T.; Haddad, T.S. *Poly.Int.,* **2000**, *49*, 453-457.

10. Haddad, T.S.; Viers, B.D.; Phillips, S.H. *J. Inorg. Organomet. Polym*., **2002**, *11* 155-164

11. Lichtenhan, J.D.; Vu, N.Q.; Carter, J.A. ; Gilman, J.W. ; Feher, F.J. *Macromolecules*, **1993**, 26, 2141-2142.

12. Baney, R.H.; Itoh, M.; Sakakibara, A.; Suzuki, T. *Chem. Rev*., **1995**, *92*, 1409-1430.

13. Lichtenhan, J.D. *Comments Inorg. Chem*., **1995**, *17*, 115-130.

14. Lichtenhan, J.D. in Polymeric Materials Encyclopedia, J.C. Salamore (ed.) CRC Press, NY, **1996** 7769-7778.

15. Li, G.Z.; Wang, L.C.; Ni, H.L.; Pittman, C.U. *J. Inorg. Organomet. Polym*., **2001**, *11* 123-154.

16. Phillips, S.H.; Haddad, T.S.; Tomczak, S.J. *Curr. Opin. Sol. State Mat. Sci.*, **2004**, *8*, 21-29.

17. Byoung-Suhk K.; Mather, P.T. *Macromolecules*, **2002**, *35*, 8378-8384.

18. Fu, B.X.; Lee, A. ; Haddad, T.S. *Macromolecules*, **2004**, *37*, 5211-5218.

19. Constable, G.S.; Lesser, A.J. ; Coughlin, E.B. *Macromolecules*, **2004**, *37*, 1276-1282.

20. Pittman, C.U.; Li, G.; Ni, H., *Macromol. Symp*., **2003**, *196,* 301-325.

21. Huang, J.; He, C.; Xiao, Y.; Mya, K.Y.; Dai, J.; Siow, Y.P. *Polymer*, **2003**, *44*, 4491-4499.

22. Kopesky, E.T.; Haddad, T.S.; Cohen, R.E.; McKinley, G.H. *Macromolecules*, **2004**, *37*, accepted for publication.

23 Zheng, L.; Hong, S.; Cardoen, G.; Burgaz, E.; Gido, S.P.; Coughlin, E.B. *Macromolecules*, **2004**, *37*, ASAP.

24. Gidden, J.; Kemper, P.R.; Shammel, E.; Fee, D.P.; Anderson, S.E.; Bowers, M.T. *Int. J. Mass Spectrom*., **2003**, *222,* 63-73.

25. Baker, E.S.; Gidden, J.; Fee, D.P.; Kemper, P.R.; Anderson, S.E.; Bowers, M.T., *Int. J. Mass Spectrom*., **2003**, *227,* 205-216.

26. Baker, E.S.; Gidden, J.; Anderson, S.E.; Haddad, T.S., Bowers, M.T. *Nano Lett.*, **2004**, *4*, 779-785.

27. von Helden, G.; Wyttenbach, T.; Bowers, M.T. *Int. J. Mass Spectrom. Ion Proc.*, **1995**, *146/147*, 349-364.

28. Gidden, J.; Wyttenbach, T.; Jackson, A.T.; Scrivens, J.H.; Bowers, M.T. *J. Am. Chem. Soc.,* **2000**, *122*, 4692-4699.

29. Gidden, J.; Wyttenbach, T.; Batka, J.T.; Weis, P.; Jackson, A.T.; Scrivens, J.H.; Bowers, M.T. *J. Am. Chem. Soc.,* **1999**, *121*, 1421-1422.

30. Gidden, J.; Wyttenbach, T.; Batka, J.T.; Weis, P.; Jackson, A.T.; Scrivens, J.H.; Bowers, M.T. *J. Am. Soc. Mass Spectrom.*, **1999**, *10*, 883-895.

31. Gidden, J.; Jackson, A.T.; Scrivens, J.H.; Bowers, M.T. *Int. J. Mass Spectrom.,* **1999***, 188*, 121-130.

32. Gidden, J.; Jackson, A.T.; Scrivens, J.H.; Bowers, M.T. *J. Am. Soc. Mass Spectrom.*, **2002**, *13*, 499-505.

33. Scrivens, J.H.; Jackson, A.T.; Yates, H.T.; Green, M.R.; Critchley, G.; Brown, J.; Bateman, R.H.; Bowers, M.T.; Gidden, J. *Int. J. Mass Spectrom. Ion Proc.,* **1997**, *165/166*, 363-375.

34. Bowers, M.T.; Kemper, P.R.; von Helden, G.; van Koppen, P.A.M., *Science,* **1993**, *260*, 1446-1451.

35. Bowers, M.T. *Accts. Chem. Res.,* **1994**, *27*, 324-332.

36. von Helden, G.; Batka, J.T.; Carlot D.; Bowers, M.T. *J. Am. Soc. Mass Spectrom.*, **1997**, *8*, 275-282; Wyttenbach, T.; Witt, M.; Bowers, M.T. *J. Am. Chem. Soc.,* **2000**, *122*, 3458-3464.

37. McDaniel E.W.; Mason, E.A. *The Mobility and Diffusion of Ions in Gases*, Wiley, NY, **1973**.

38. Kollman, P.A.; *et. al*., AMBER6, University of California at San Francisco, **1999**.

39. Sun, H. *Macromolecules,* **1995***, 28*, 701-712.

40. Sun H.; Rigby,D. *Spectrochim. Acta,* **1997***, A 53*, 1301-1323.

41. Bassindale, A.R.; Pourny, M.; Taylor, P.G.; Hursthouse, M.B.; Light, M.E. *Angew. Chem., Int. Ed.,* **2003**, *42,* 3488-3490.

42. Itami, Y.; Marciniec, B.; Kubicki, M. *Chem. Eur. J.*, **2004,** *10*, 1239-1248.

43. HyperChem(TM) Professional 7.1, Hypercube, Inc., 1115 NW 4th Street, Gainesville, Florida 32601, USA

44. Shvartsburg, A.A.; Jarrold, M.F. *Chem. Phys. Lett.,* **1996**, *261*, 86-91.

45. Melsch, M.F.; Hunter, J.M.; Svartsburg, A.A.; Schatz, G.C.; and Jarrold, M.F. *J. Phys. Chem.*, **1996**, *100*, 16082-16086.

46. See, for example, Bernstein, S.L. ; Wyttenbach, T. ; Baumketner, A. ; Shea, J-E. ; Betan, G. ; Teplow, D.B. ; Bowers, M.T., *J. Am. Chem. Soc.* (in press).

47. Pyun, J.; Matyjasewski, K., *Macromolecules*, **2000**, *333*, 217-220.

48. Bryan Coughlin, private communication.

FIGURE CAPTIONS

1. Three common POSS materials: A fully condensed cage with eight methyl groups (Me_8T_8), an incompletely condensed trisilanol ($Cp_7T_7(OH)_3$) useful in making a polymerizable POSS with a single functionality; and a Cp_7T_8(propylmethacrylate).

2. A homopolymer of a POSS-propylmethacrylate terminated at both ends with hydrogens.

3. MALDI-TOF mass spectrum of $[(PMA)Cp_7T_8]_x{\cdot}Na^+$ oligomers.

4. Arrival time distributions (ATDs) of $[(PMA)Cp_7T_8]_x{\cdot}Na^+$ for x = 1, 2, 3 obtained at a drift cell temperature of 300K. See text for "cis" and "trans" labeling for x = 2.

5. Plots of cross-section vs. energy for $(PMA)Cp_7T_8{\cdot}Na^+$. Each point represents one theoretical structure generated by the simulated annealing method. The average cross-section is based on all structures since the relative energies of these structures are very similar.

6. A typical structure calculated for $(PMA)Cp_7T_8{\cdot}Na^+$. The cyclopentyl carbon atoms are white, the methacrylate group carbon atoms are gray, silicon is green, carbonyl and POSS oxygen atoms are red and sodium is yellow (hydrogen atoms have been omitted for clarity).

7. Scatter plot of cross-section vs. energy for $[(PMA)Cp_7T_8]_2{\cdot}Na^+$. Each point represents one theoretical structure generated by the simulated annealing method. Minimum energy structures belonging to the trans family are closed circles (●), those in the extended trans family are x's (∗), and those belonging to the cis family are open circles (o).

8. The lowest-energy structures calculated for the $[(PMA)Cp_7T_8]_2{\cdot}Na^+$. The sodium ion is shown for both structures and coordinates to a different number of oxygens in more compact versus less compact structures. The cyclopentyl groups capping the silicon atoms are omitted for clarity. The methacrylate group carbon atoms are gray, silicon is green, carbonyl and POSS oxygen atoms are red and sodium is yellow.

9. The $[(PMA)Cp_7T_8]_3{\cdot}Na^+$ oligomer (terminated at both ends with hydrogens) has two possible regioisomers. In a staggered conformation, the POSS groups (R) bonded to the two chiral centers are either syndiotactic (left) or isotactic (right) with respect to each other.

10. The lowest-energy structures calculated for the $[(PMA)Cp_7T_8]_3{\cdot}Na^+$ syndiotactic isomer. The sodium ion is typically coordinated to a cage face and one or more carbonyl oxygens of the oligomer backbone. The cyclopentyl groups capping the silicon atoms are omitted for clarity, the methacrylate group carbon atoms are gray, silicon is green, carbonyl and POSS oxygen atoms are red and sodium is yellow.

11. The lowest-energy structures calculated for a Na+ cationized a) 8-PMA and b) POSS 8-PMA. The cyclopentyl groups capping the silicon atoms are omitted for clarity. The methacrylate group carbon atoms are gray, silicon is green, carbonyl and POSS oxygen atoms are red and sodium is yellow.

12. Stereoscopic view of the lowest-energy structure calculated for the $[(PMA)Cp_7T_8]_8{\cdot}Na^+$. The cyclopentyl groups capping the silicon atoms are omitted for clarity. The "backbone" carbon atoms rendered as tubular are black, all other carbons are blue, silicon is green, carbonyl and POSS oxygen atoms are red and sodium is yellow.

Table 1. Collision Cross-Sections (Å^2) for $[(PMA)Cp_7T_8]_x{\cdot}Na^+$ Oligomers

Oligomer	Experimental	Theory[a]	Theory[a] (without Na^+)	% Experimental Abundance
x = 1	248	252	-	100
x = 2	378	377 (trans)	380	20
	402	393 (cis and extended trans)	400	80
x = 3	539	540 (syndiotactic)	548	100
		555 (isotactic)	-	

a) Calculated average cross-sections (see text).

Table 2. Collision Cross-Sections (Å^2) for $[(PMA)Cp_7T_8]_2{\cdot}Na^+$ Conformers

Conformer[a]	**Experimental Average (Å^2)**	**Theory**[b] **(0 - 5 kcal/mol)**	**Theory**[b] **(5-10 kcal/mol)**
cis	402	393(3)	394(7)
trans $_{ext}$		391 (8)	391(10)
trans	378	374 (4)	381(4)

a) See Figure 8. b) Calculated average cross-sections (see text) as a function of relative energy.